Inorganic Chemistry

Article

pubs.acs.org/IC

High Nuclearity (Octa-, Dodeca-, and Pentadecanuclear) Metal (M = Co^{II}, Ni^{II}) Phosphonate Cages: Synthesis, Structure, and Magnetic Behavior

Javeed Ahmad Sheikh, Amit Adhikary, Himanshu Sekhar Jena, Soumava Biswas, and Sanjit Konar*

Department of Chemistry, IISER Bhopal, Bhopal-462066, India

Supporting Information

ABSTRACT: The synthesis, structural characterization, and magnetic property studies of five new transition metal (M = Co, Ni) phosphonate-based cages are reported. Three substituted phenyl and benzyl phosphonate ligands [RPO_3H_2; R_1 = *p-tert*-butylbenzyl, R_2 = *p-tert*-butylphenyl, R_3 = 3-chlorobenzyl] were synthesized and employed to seek out high-nuclearity cages. Complexes **1**−**3** are quasi-isostructural and feature a dodecanuclear metal-oxo core having the general molecular formula of $[M_{12}(\mu_3\text{-}OH)_4(O_3PR)_4(O_2C^tBu)_6(HO_2C^tBu)_6(HCO_3)_6]$ {M = Co, Ni and R = R_1 for **1** (Co_{12}), R_2 for **2**, **3** (Co_{12}, Ni_{12})}. The twelve metal centers are arranged at the vertices of a truncated tetrahedron in a manner similar to Keggin ion. Complex **4** is an octanuclear nickel phosphonate cage $[Ni_8(\mu_3\text{-}OH)_4(OMe)_2(O_3PR_1)_2(O_2C^tBu)_6(HO_2C^tBu)_8]$, and complex **5** represents a pentadecanuclear cobalt phosphonate cage, $[Co_{15}(chp)_8(chpH)(O_3PR_3)_8(O_2C^tBu)_6]$, where chpH = 6-chloro-2-hydroxypyridine. Structural investigation reveals some interesting geometrical features in the molecular cores, which may provide new models in single molecular magnetic materials. Magnetic property measurements of compounds **1**−**5** indicate the coexistence of both antiferromagnetic and ferromagnetic interactions between magnetic centers for all cages.

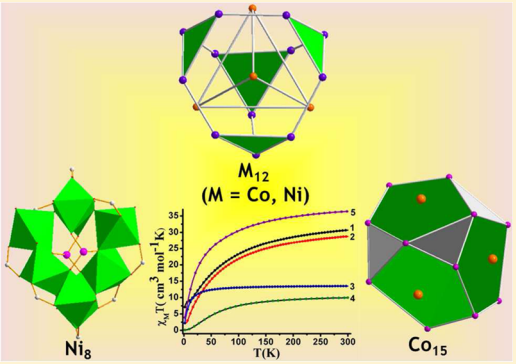

Polynuclear transition metal cages and clusters have emerged as an active area of research in the recent past, owing to their immense technological applications,[1] relevance in biological systems,[2] and also because of aesthetically pleasing structures.[3] On the other hand, molecular magnetic materials based on discrete transition-metal aggregates have received much attention, as they typically display properties of a single molecular magnet.[4] Numerous transition metal cluster/cage compounds reported in the literature have been synthesized using carboxylates[5] or alkoxides[6] as ligand. Phosphonate ligands possessing three O donors could be an ideal choice for the synthesis of polynuclear cages. However, because of their multidentate coordination capability, phosphonates tend to generate insoluble metal complexes.[7] This problem has been addressed by the use of preformed cages or the introduction of ancillary ligands, and considerable progress has been achieved by the groups of Winpenny,[8] Clearfield,[9] Chandrasekhar,[10] and others[11,12] in exploring metal-phosphonate cage compounds as magnetic materials. However, most of these phosphonate cages reported so far bear core structures of irregular geometrical pattern, and cages with regular geometrical cores are relatively rare.[8j,10,12,13,24] Regular geometry in polynuclear paramagnetic cores is of importance from a magnetic point of view as it is easier to model magnetic data for smaller symmetry-related subunits, and it also helps to understand magnetic behavior from a structural point of view.

In our recent work, we have reported a dodecanuclear and a pentadecanuclear cobalt phosphonate cage featuring butterfly and distorted cubic cores, respectively, and also an octadecanuclear Cu-pyrazolate-phosphonate nanocage.[13] In our efforts to explore new types of transition-metal-based phosphonate cages using different phosphonic acids, we are able to isolate and characterize a series of complexes having three different nuclearities. Herein, we report the synthesis, structural, and magnetic studies of five new phosphonate-based Co^{II}/Ni^{II} cage compounds, of which three are structurally analogous dodecanuclear transition metal (M = Co, Ni) phosphonate cage compounds having the general molecular formula of $[M_{12}(\mu_3\text{-}OH)_4(O_3PR)_4(O_2C^tBu)_6(HO_2C^tBu)_6(HCO_3)_6]$, where M = Co, Ni and R = R_1 (*p-tert*-butylbenzyl) for compound **1** (Co_{12}) and R_2 (*p-tert*-butylphenyl) for compounds **2** and **3** (Co_{12} and Ni_{12}). The remaining two compounds include an octanuclear Ni phosphonate cage of molecular formula $[Ni_8(\mu_3\text{-}OH)_4(OMe)_2(O_3PR_1)_2(O_2C^tBu)_6(HO_2C^tBu)_8]$ (**4**) and a pentadecanuclear Co phosphonate cage of molecular formula $[Co_{15}(chp)_8(chpH)(O_3PR_3)_8(O_2C^tBu)_6]$ (R_3 = 3-chlorobenzyl, chpH = 6-chloro-2-hydroxypyridine) (**5**). The phosphonic acid ligands (Scheme 1) were synthesized following the Michaelis−Arbuzov reaction[14] from their corresponding bromides.

Received: October 24, 2013
Published: January 17, 2014

dx.doi.org/10.1021/ic402673v | *Inorg. Chem.* 2014, 53, 1606−1613

Scheme 1. Schematic Drawing of the Phosphonic Acid Ligands

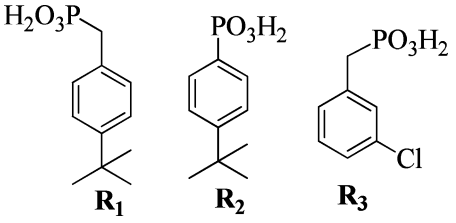

Magnetic measurements and bond valence sum (BVS) calculations authenticate that metal centers in all the mentioned molecules are at +2 oxidation state, as required for the charge balances (Supporting Information, Table S1).[15] Magnetic property measurements of compounds **1**−**5** indicate the coexistence of both antiferromagnetic and ferromagnetic interactions between magnetic centers for all cages.

EXPERIMENTAL SECTION

X-ray Crystallography. Data collection of the compounds were performed at 130−140 K on a Bruker Smart CCD-1000 diffractometer with Mo Kα (λ = 0.710 73 Å) radiation using a cold nitrogen stream (Oxford). Data reduction and cell refinements were performed with the SAINT program[16] and the absorption correction program SADABS[17] was employed to correct the data for absorption effects. Crystal structures were solved by direct methods and refined with full-matrix least-squares (SHELXTL-97)[18] with atomic coordinates and anisotropic thermal parameters for all non-hydrogen atoms. Crystals of compounds **2**−**5** were notably poorly diffracting. The lower angle reflection data consequences a poor data to parameter ratio and in anisotropic refinement some atoms became anisotropic displacement parameters (ADPs). The thermal parameters of all the carbon atoms were restrained to approximately the same values using the XShell "rigid bond displacement" (DELU, Sigma 0.05), "isotropic displacement" (ISOR, Sigma 0.8) command. The structures of complexes **1**−**5** contain solvent-accessible voids; hence, the SQUEEZE[19] module of the program suite PLATON[20] was used to generate a fresh reflection file. The crystallographic data are summarized in Table 1.

Materials and Methods. All the complexes were synthesized from the starting materials $[Co_2(\mu\text{-}OH_2)(O_2C^tBu)_4]\cdot(HO_2C^tBu^tBu)_4]$, Co_2 or $[Ni^{II}_2(\mu\text{-}OH_2)(O_2C^tBu)_4(HO_2C^tBu)_4]$, Ni_2 which were made by literature methods.[21,22] The phosphonate ligands were synthesized following previously reported procdures.[8c,12] Other reagents were used as received from Sigma Aldrich without any further purification. Magnetic susceptibility and magnetization measurements were carried out on a Quantum Design SQUID-VSM magnetometer. Direct current (DC) magnetic measurements were performed with an applied field of 1000 G in the 1.8−300 K temperature range. Alternating current (AC) magnetic susceptibilities were performed in a 3.5 G field oscillating at 1−780 Hz in the 1.8−10 K range. BVS calculations were done following the procedure given by Liu and Thorpe.[15] Powder X-ray diffraction (PXRD) data was obtained with PANanalytical instrument using Cu Kα radiation, and data for thermogravimetric analysis (TGA) was collected on a PerkinElmer TGA 4000.

Synthesis. *$[Co_{12}(\mu_3\text{-}OH)_4(HCO_3)_6(O_3PR)_4(O_2C^tBu)_6(HO_2C^tBu)_6]$ (R = p-tert-Butylbenzyl) (1).* $[Co_2(\mu\text{-}OH_2)(O_2C^tBu)_4]\cdot(HO_2C^tBu)_4]$ (100 mg, 0.1 mmol) and *p-tert*-butylbenzylphosphonic acid (23 mg, 0.1 mmol) were taken in CH_3CN (8 mL) and stirred at ambient temperature for a few minutes. This was followed by the addition of NEt_3 (20 mg, 0.2 mmol) (Et = ethyl), and after further stirring for a few minutes, the contents were transferred into a Teflon-lined steel autoclave and heated at 150 °C for 18h and then cooled to room temperature. The resulting solid product was filtered, and the deep-blue solution was kept in a 15 mL vial at 4 °C for ca. 2 d. Purple block-shaped crystals suitable for X-ray diffraction were collected by filtration. Yield 35 mg, 36%, based on Co_2. IR (KBr, cm^{-1}); 3467 (b), 3198 (b), 2961 (s), 2870 (s), 2372 (s), 2171 (w), 1932 (b), 1629 (b), 1513 (m), 1458 (m), 1401 (vs), 1364 (s), 1265 (s), 1096 (m), 972 (b), 844 (vs), 765 (s), 732 (s), 695 (m), 614 (m).

$[Co_{12}(\mu_3\text{-}OH)_4(HCO_3)_6(O_3PR)_4(O_2C^tBu)_6(HO_2C^tBu)_6]$ (R = p-tert-Butylphenyl) (2). This compound was synthesized following a similar procedure as for **1**, but *p-tert*-butylphenylphosphonic acid (22 mg, 0.1 mmol) was used here instead of *p-tert*-butylbenzylphosphonic acid. Purple block-shaped crystals suitable for X-ray diffraction were collected by filtration after 4 d. Yield 42 mg, 43.5%, based on Co_2.

Table 1. Crystal Data and Structure Refinement for Complexes 1−5

	1	2	3	4	5
formula	$C_{110}H_{176}Co_{12}O_{58}P_4$	$C_{115}H_{172}Co_{12}N_4O_{60}P_4$	$C_{114}H_{165}N_3Ni_{12}O_{65}P_4$	$C_{94}H_{141}Ni_8O_{40}P_2$	$C_{140}H_{118}Cl_{18}Co_{15}N_{12}O_{48}P_8$
formula weight	3257.55	3401.62	3445.72	2442.54	4506.28
T (K)	140(2)	130(2)	130(2)	130(2)	130(2)
wavelength (Å)	0.71073	0.71073	0.71073	0.71073	0.71073
space group	$P\bar{4}2_1c$	$C2/c$	$P\bar{3}c1$	$C2/c$	$C2/c$
crystal system	tetragonal	monoclinic	hexagonal	monoclinic	monoclinic
a/Å	21.5512(18)	17.3222(9)	19.7023(5)	57.000(7)	20.011(3)
b/Å	21.5512(18)	30.933(2)	19.7023(5)	16.0479(18)	28.907(4)
c/Å	19.1984(19)	30.4764(17)	52.319(2)	30.275(3)	30.350(6)
α/deg	90.00	90.00	90.00	90.00	90.00
β/deg	90.00	96.517(3)	90.00	105.678(6)	93.332(12)
γ/deg	90.00	90.00	120.00	90.00	90.00
V/Å^3	8916.8(17)	16224.4(16)	17588.5(9)	26663(5)	17527(5)
Z	2	4	4	8	4
D_{calcd} (g cm^{-3})	1.213	1.393	1.298	1.217	1.708
μ (mm^{-1})	1.189	1.312	1.366	1.196	1.806
F(000)	3368	7016	7128	10232	9028
θ_{min}, θ_{max} (deg)	1.34, 27.49	2.00, 25.29	2.07, 26.79	0.74, 32.22	1.38, 25.37
reflections collected	10 246	14 779	12 529	47 156	16 090
unique reflections	9700	10 861	10 688	40 309	15 320
R_1, wR_2 ($I \geq 2\sigma(I)$)[a]	0.0566, 0.1796	0.1096, 0.2878	0.0823, 0.2082	0.1228, 0.2791	0.0838, 0.2448
goodness of fit (GOF) on F^2	1.002	1.134	1.213	1.119	1.049

[a] $R_1 = \sum||F_o| - |F_c||/\sum|F_o|$. $wR_2 = [\sum[w(F_o^2 - F_c^2)^2]/\sum[w(F_o^2)^2]]^{1/2}$.

dx.doi.org/10.1021/ic402673v | Inorg. Chem. 2014, 53, 1606−1613

IR (KBr, cm^{-1}); 3432 (b), 3179 (b), 2963 (s), 2871 (s), 2374 (m), 2171 (w), 1623 (b), 1547 (m), 1485 (vs), 1458 (m), 1429 (s), 1379 (m), 1363 (m), 1270 (s), 1231 (vs), 1205 (m), 1098 (m), 1029 (s), 990 (vs), 898 (vs), 830 (s), 809 (m), 788 (s), 755 (s), 670 (w), 628 (s).

*$[Ni_{12}(\mu_3\text{-}OH)_4(HCO_3)_6(O_3PR)_4(O_2C^tBu)_6(HO_2C^tBu)_6]$ (R = p-tert-Butylphenyl) (**3**).* This compound was synthesized following a similar procedure as for **2**, but $[Ni^{II}_2(\mu\text{-}OH_2)(O_2C^tBu)_4(HO_2C^tBu)_4]$ (100 mg, 0.1 mmol) was used instead of $[Co_2(\mu\text{-}OH_2)(O_2C^tBu)_4]\cdot(HO_2C^tBu)_4]$. Deep-green cubic crystals suitable for X-ray diffraction were collected by filtration after 4 d. Yield 54 mg, 55.96%, based on Ni_2. IR (KBr, cm^{-1}); 3423 (b), 3180 (b), 2958 (s), 2870 (m), 2369 (m), 1670 (s), 1602 (s), 1508 (m), 1483 (vs), 1458 (m), 1419 (s), 1373 (s), 1360 (m), 1270 (m), 1229 (vs), 1122 (s), 1090 (vs), 1028 (s), 991 (vs), 879 (b), 834 (m), 785 (s), 750 (s), 611 (vs), 588 (s), 530 (s).

*$[Ni_8(\mu_3\text{-}OH)_4(OMe)_2(O_3PR)_2(O_2C^tBu)_6(HO_2C^tBu)_8]$ (R = p-tert-Butylbenzyl) (**4**).* This compound was synthesized following a similar procedure as for **3**; however, *p-tert*-butylbenzylphosphonic acid (23 mg, 0.1 mmol) was used here, and the reaction was done under ambient conditions. The final product was dissolved in toluene and layered with methanol. Green cubic crystals suitable for X-ray diffraction were collected by filtration after a few days. Yield 32 mg, 33.17%, based on Ni_2. IR (KBr, cm^{-1}); 3436 (b), 3179 (b), 2966 (s), 2874 (m), 2593 (m), 2372 (m), 2345 (m), 2170 (w), 1600 (b), 1483 (s), 1458 (m), 1405 (s), 1374 (m), 1322 (s), 1208 (s), 1110 (b), 1000 (s), 902 (m), 872 (m), 841 (m), 787 (s), 614 (s).

*$[Co_{15}(chp)_8(chpH)(O_3PR)_8(O_2C^tBu)_6(CH_3CN)_3]\cdot(CH_3CN)$ (R = 3-Chlorobenzyl) (**5**).* $[Co^{II}_2(\mu\text{-}OH_2)(O_2C^tBu)_4]\cdot(HO_2C^tBu)_4$, (100 mg, 0.1 mmol), 3-chlorobenzylphosphonic acid (23 mg, 0.1 mmol), and 6-chloro-2-hydroxypyridine (13 mg, 0.1 mmol or 39 mg, 0.3 mmol) were taken in CH_3CN (8 mL) and stirred at ambient temperature a for few minutes. This was followed by the addition of NEt_3 (30 mg, 0.3 mmol), and after further stirring for a few minutes the contents were transferred into a Teflon-lined steel autoclave and heated at 150 °C for 18h and then cooled to room temperature. The resulting solid product was filtered, and the deep-blue solution was kept in a 15 mL vial at 4 °C for ca. 2 d. Deep-blue block-shaped crystals suitable for X-ray diffraction were collected by filtration. Yield 62 mg, 64.25%, based on Co_2. IR (KBr, cm^{-1}); 3448 (b), 3186 (b), 2958 (s), 2371 (m), 2345 (w), 2167 (w), 1596 (s), 1559 (m), 1508 (m), 1482 (w), 1445 (m), 1420 (w), 1341 (m), 1229 (s), 1162 (m), 1089 (s), 1001 (s), 978 (m), 939 (s), 876 (m), 793 (vs), 737 (s), 700 (s), 681 (s), 616 (vs).

RESULTS AND DISCUSSION

Synthetic Aspects. Reaction of the cobalt and nickel pivalate dimers with phosphonic acids generated five high-nuclearity phosphonate cages. The structures of the final products were not profoundly affected by changing the phosphonate ligands as we ended up with the M_{12} (M = Co, Ni) phosphonate cages under solvothermal conditions (150 °C). However, introduction of the coligand along with the phosphonate ligand in the reaction resulted in a completely different molecule with higher nuclearity (pentadecanuclear) and less symmetry. Interestingly, we obtained an octanuclear Ni phosphonate cage under ambient conditions with the ligand ($R_1PO_3H_2$) that gave a Co_{12} cage at 150 °C. The bulk phase PXRD pattern of complexes **1**−**5** is in good agreement with the simulated ones based on single crystal data, indicating the purity of the as-synthesized compounds (Supporting Information, Figures S2−S6). The discrepancies between the experimental and simulated powder X-ray diffraction patterns might be due to the partial loss of solvent molecules from the crystal lattice. TGA of all the complexes reveals a weight loss of around 10% up to 150 °C that may be assigned to the coordinated and noncoordinated solvent molecules. Further weight loss of around 15−20% in the temperature range of 200−300 °C probably corresponds to the aromatic ligands, after which the complexes decompose completely (Supporting Information, Figure S7).

Structural Description. X-ray crystallography studies show that complexes **1**−**3** are quasi-isostructural, which can be best described as an M_{12} (M = Co, Ni) central core coated on the exterior by a hydrophobic sheath of alkyl or aryl groups (Figure 1, Supporting Information, Figure S1, and Figure 2, respectively). The core is made of 12 octahedral Co^{II}/Ni^{II} centers held together by 4 μ_3−hydroxo groups, 4 doubly deprotonated phosphonate ligands, 12 carboxylates (6 protonated and deprotonated each), and 6 monoprotonated carbonates. In all the complexes, the phosphonate ligands bind

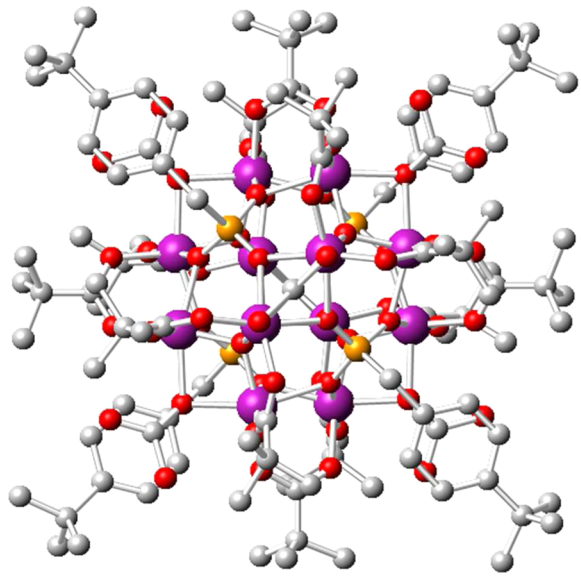

Figure 1. Ball-and-stick model showing molecular structure of **1** in the crystal. Color code: purple, cobalt; orange, phosphorus; red, oxygen; gray, carbon; Hydrogen atoms are omitted for clarity.

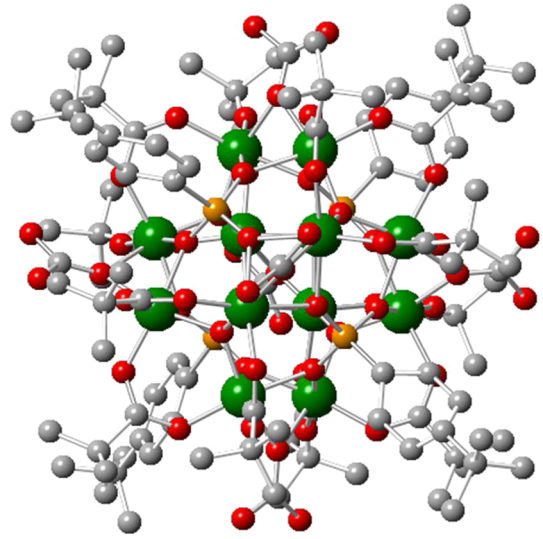

Figure 2. Ball-and-stick model showing molecular structure of **3** in the crystal. Color code: green, nickel; orange, phosphorus; red, oxygen; gray, carbon; Hydrogen atoms are omitted for clarity.

dx.doi.org/10.1021/ic402673v | Inorg. Chem. 2014, 53, 1606−1613

in the 6.222 mode as per Harris notation (Supporting Information, Scheme S1).[23]

The pivalate and carbonate ligands surround the periphery of the complexes binding in 2.11 and 2.200 modes, respectively. The core of the molecules can be better described as an ε-Keggin (Figure 3a). The core structures of compounds **1**−**3**

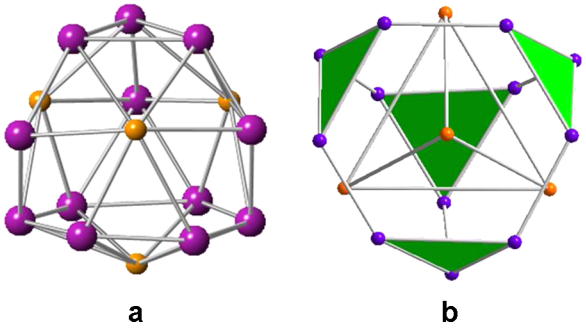

Figure 3. (a) Core structure of **1**−**3**, displaying ε-Keggin-like view. Color code same as in Figure 1. (b) "Stick"-type view of the core after removing all atoms except metal and phosphorus.

strongly resemble to the Ni^{II} phosphonate cage reported by Winpenny et al.[24] The bond distances and bond angles around the metal centers fall in a range similar to the reported compound. Removing all atoms, excluding the metal centers and phosphorus, and connecting the metal centers and phosphorus through imaginary lines results in a geometry where each phosphorus atom is surrounded by six cobalt ions, and thereby four hexagonal and four trigonal faces are formed where all the vertices are occupied by metal ions (Figure 3b). The four hexagons share edges, and the triangular faces have central μ_3-OH groups. Metal−metal distances within the trimeric unit are in the range of 3.23−3.46 Å, and between two trimeric units they are in the range of 2.88−3.08 Å.

The interconnection of phosphorus atoms of the ligands resulted in a tetrahedral geometry (T_d) where four phosphorus atoms (P_4) occupied its vertices with an average P−P distance of 5.16 Å. It can be seen that four metal triangles engulf the P_4 tetrahedra and this feature makes the structure unique and aesthetically pleasing. The phosphorus atoms of the ligand are somewhat above the plane of the hexagon generated by joining cobalt triangles. There are four axes of C_3, each at the vertex of P_4 T_d, running through the center of each Co_3 triangular unit at the opposite end (Figure 3b). Nine mirror planes are also present along each edge of the hexagonal faces.

The molecular structure of complex **4** consists of eight octahedral Ni^{II} centers held together by two phosphonate ligands, both binding in a 5.221 mode[23] (Figure 4). There are also eight pivalate groups binding in a 2.11 mode. Two butterfly-like Ni_4 subunits are formed via pivalate and hydroxy bridging. The phosphonate ligands are located trans to each other, thus holding together two $\{Ni_4(\mu\text{-}OH)_2\}$ butterflies of Ni^{II} ions.

Four pivalate ligands bridge wing-body nickel centers within the butterflies; two of them bridge body−body Ni, and two of them bridge between the butterflies. Two methoxide molecules are also found bridging between the nickel butterflies. The distances between two adjacent Ni^{II} centers are in the range of 2.89−3.69 Å. The core structure of this phosphonate cage resembles the Ni^{II} phosphonate cage reported earlier.[24] The bond distances and bond angles around the metal centers fall in

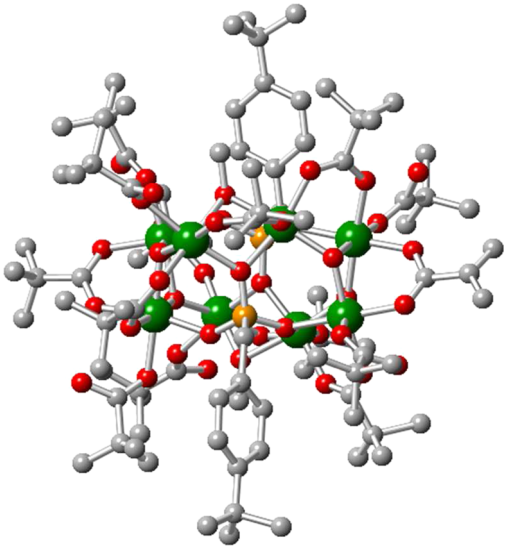

Figure 4. Molecular structure of **4** in the crystal. Color code same as in Figure 2.

a range similar to the reported compound. The core structure of **4**, after removing the organic ligands for clarity, is shown in Figure 5.

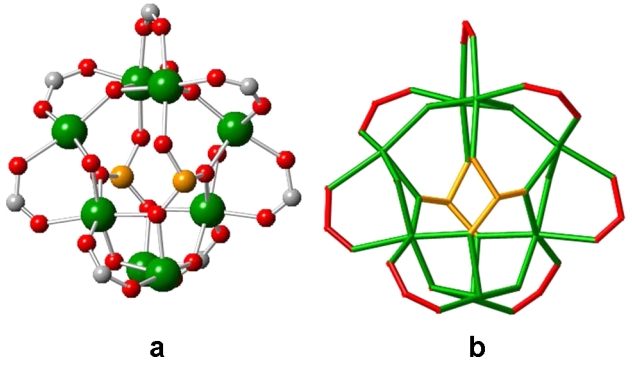

Figure 5. (a) Butterfly-shaped molecular core of **4**. Color code same as in Figure 2. (b) Stick view of core of **4**. Bond colors: Ni−O, green; P−O, orange; C−O, red.

Structural studies reveal that complex **5** contains an inorganic core composed of 15 Co^{II} ions that are held together by bridging oxygen atoms from eight doubly deprotonated phosphonates and six carboxylate ligands (Figure 6). Of the 15 Co^{II} centers, 9 centers exhibit an octahedral geometry, 5 centers show a tetrahedral geometry, and 1 center exhibits a square-pyramidal arrangement. Six of the eight phosphonate ligands show the 5.221 bridging mode, and another two ligands are exhibiting the 3.11 mode as per Harris notation.[23] The complex is also comprised of nine 6-chloro-2-hydroxypyridine coligands that bind with cobalt sites via nitrogen as well as oxygen.

Organic parts of the ligands are pointed toward the outer periphery of the molecule. Six pivalates are also present and bridge in 2.11 mode. Metal and phosphorus tethered by oxygen atoms give a distorted cubic view of the core of the complex (Figure 7a). Further, removing all the atoms except Co and P centers and connecting them through imaginary lines resulted in an interesting perspective of the structure (Figure 7b). Here each phosphorus (except P9) bears five Co^{II} centers as nearest

dx.doi.org/10.1021/ic402673v | Inorg. Chem. 2014, 53, 1606−1613

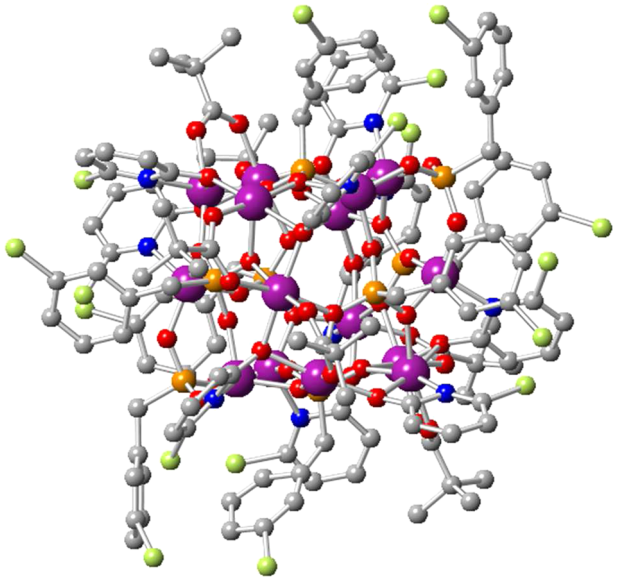

Figure 6. Molecular structure of **5** in the crystal. Color code same as in Figure 1, with the addition of chlorine, dark green.

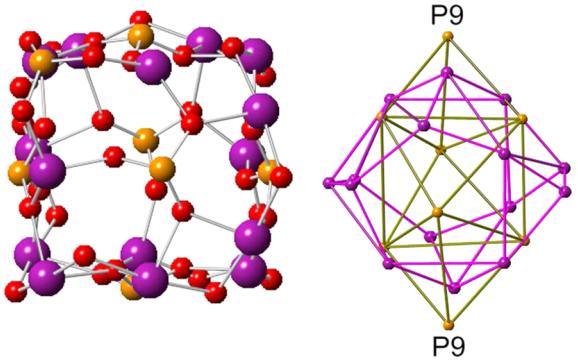

Figure 7. (a) Core structure of **5**. Color code same as in Figure 1. (b) Stick-type view of the core after removing all atoms except Co and P. Bond colors: M−M, purple; P−P, green.

neighbors, and thereby a pentagonal unit is formed. Each pentagon shares three vertices and an edge with its adjoining pentagons and thereby forms a new type of geometry having a total of six pentagonal and eight triangular faces, with each of the vertices occupied by a metal center. A representative polyhedral view of the core can be seen after the removal of two phosphorus sites, P9 and P9A (Figure 8). The remaining two phosphonate groups cap two of the opposite triangular faces and observe a 3.111 bridging mode.[23] The average distance of cobalt ions of the hexagonal faces is 3.0 Å, and that of the triangular faces is 3.32 Å.

Magnetic Properties. The variable-temperature magnetic susceptibility data of complexes **1**−**5** were collected in the temperature range of 1.8−300 K under a field of 0.1 T. The DC susceptibilities are shown in the form of $\chi_M T$ (χ_M is molar magnetic susceptibility) as a function of temperature. AC susceptibility studies show no slow relaxation of magnetization in any of these compounds; hence, none of them are single-molecule magnets. The angle dependency of magnetic exchange interactions for compounds **3** and **4** is given in the

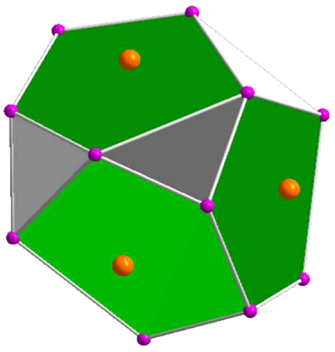

Figure 8. Polyhedral view of the core of complex **5**.

Supporting Information, Table S2. The data for **3** and **4** were fitted assuming isotropic spin Hamiltonian.[25]

The room temperature $\chi_M T$ values of 30.68 cm^3 K mol^{-1} and 29.10 cm^3 K mol^{-1} for compounds **1** and **2**, respectively, can be explained on the basis of the orbital contribution of Co^{II}, which is known to be significant in an octahedral field (Table 2).[8e,26]

Table 2. Magnetic Susceptibility Data $\chi_M T$ (cm^3 K mol^{-1}) of Complexes 1, 2, and 5

compound	expected $\chi_M T$ (spin only)	expected $\chi_M T$ (spin +orbital)	experimental $\chi_M T$
1	22.50	40.23	30.68
2	22.50	40.23	29.10
5	28.12	50.28	36.15

As the temperature is lowered from 300 K, the $\chi_M T$ value decreases gradually until it reaches 7.09 cm^3 K mol^{-1} and 3.18 cm^3 K mol^{-1} at 1.8 K for **1** and **2**, respectively. The gradual decline at higher temperatures may be attributed to the presence of intramolecular antiferromagnetic interaction in the molecules.[26]

The M/N μ**B** versus H plots for compounds **1** and **2** from 2 to 10 K (inset of Figures 9 and 10, respectively) show a steady increase with field that reaches 9.14 and 9.18 μ**B**, respectively, at 7 T and 2 K without any saturation. These lower values are inconsistent with 12 uncoupled Co^{II} ions (36 μ**B**, g = 2). Instead these values correspond to three Co^{II} ions of one trimeric unit, and it can be assumed that the Co^{II} ions are

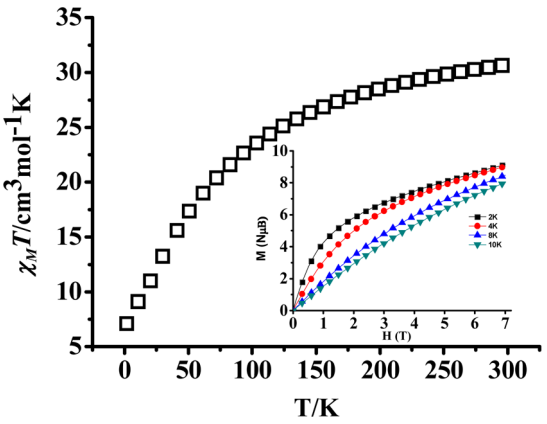

Figure 9. Temperature dependence of $\chi_M T$ measured at 0.1 T. Magnetization curves (inset graphs) measured at 2−10 K for complex **1**.

dx.doi.org/10.1021/ic402673v | Inorg. Chem. 2014, 53, 1606−1613

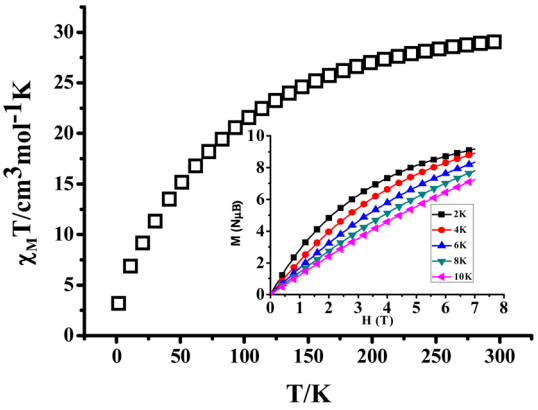

Figure 10. Temperature dependence of $\chi_M T$ measured at 0.1 T. Magnetization curves (inset graphs) measured at 2−10 K for complex **2**.

strongly antiferromagnetically coupled even at higher field, which reduced the overall magnetic moment.[8c] The unsaturated behavior of the plots can be explained by assuming strong magnetic anisotropy of the ions present with high nuclearity, resulting in many spin states populated at low temperature.[26]

The room-temperature $\chi_M T$ value for compound **3** is 13.28 cm^3 K mol^{-1}, which is close to the expected value (13.23 cm^3 K mol^{-1}) for twelve isolated Ni^{II} ions (g = 2.1) (Figure 5). The $\chi_M T$ value decreases gradually from room temperature to 12.91 cm^3 K mol^{-1} at 53 K and then sharply to 1.99 cm^3 K mol^{-1} at 1.8 K (Figure 12). The magnetic properties of compound **3** are

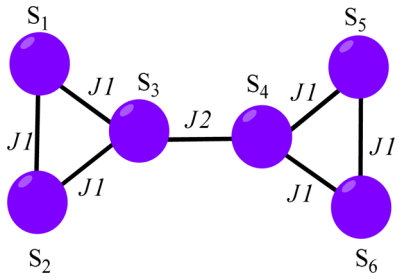

Figure 11. Model used for the data fitting of compound **3**. Balls represent metal centers, and lines represent connectivity between two metal centers.

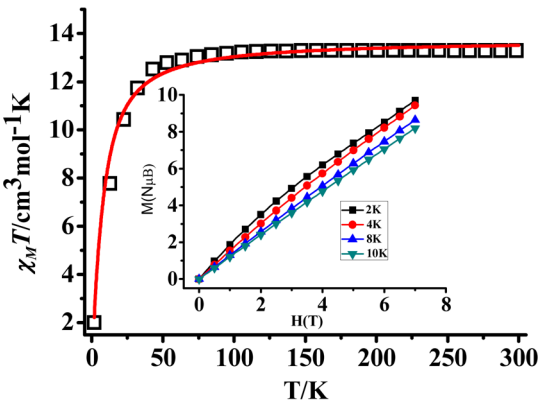

Figure 12. Temperature dependence of $\chi_M T$ measured at 0.1 T. The red solid line is the best fit obtained. Magnetization curves (inset graphs) measured at 2−10 K for complex **3**.

in good agreement with the similar phosphonate cage reported earlier.[24] The magnetic interactions for **3** were modeled after taking symmetry-related unit (half molecule) into consideration (Figure 11) with the Hamiltonian given in eq 1, neglecting any coupling between the two six-centered halves because of the complexity in the structure. This matches well with the experimental result, giving the values of g = 2.14, $J1$ = −3.1 cm^{-1}, and $J2$ = 2.5 cm^{-1}. The magnetic exchange pathways can be explained on the basis of the Ni−O−Ni bond angle. If the Ni−O−Ni angle is smaller than 99°, interactions are ferromagnetic; larger values correspond to antiferromagnetic interactions.[24,27]

$$\mathbf{H} = -J1(S_1S_2 + S_2S_3 + S_3S_1 + S_4S_5 + S_4S_6 + S_5S_6) - J2(S_3S_4) - g\mu\mathbf{BH}.\sum_{i=1}^{6} S_i \quad (1)$$

Antiferromagnetic interactions are observed via $J1$ exchange pathways that can be justified by the Ni−O−Ni angle of 117−119°. Since the Ni−O−Ni angle is around 87° via $J2$, it yields ferromagnetic interactions. This would lead to a spin frustration situation for each triangle (S_1−S_3 and S_4−S_6).[8c] The M/N μ**B** versus H plot shows no saturation even at a higher field of 7 T. This behavior is analogous to that of compounds **1** and **2** and can be explained with similar assumptions.

The room temperature $\chi_M T$ value for compound **4** is 10.0 cm^3 K mol^{-1}, which is near the expected value (9.94 cm^3 K mol^{-1}) for eight isolated Ni^{II} ions (g = 2.2) (Figure 13), and the

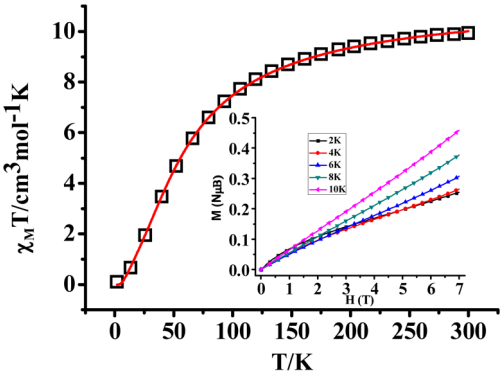

Figure 13. Temperature dependence of $\chi_M T$ measured at 0.1 T. The red solid line is the best fit obtained. Magnetization curves (inset graphs) measured at 2−10 K for complex **4**.

$\chi_M T$ value gradually decreases with temperature to reach the value of 0.1 cm^3 K mol^{-1} at 1.8 K. The magnetic properties of compound **4** are quite similar to those of the phosphonate cage reported earlier.[24] The magnetic behavior was modeled with the Hamiltonian given in eq 2 (Figure 14). The first exchange pathway ($J1$) is assigned to the four Ni...Ni vectors which represent the two body−body contacts within the butterflies.[24] The second pathway ($J2$) is assigned to the eight body−wing contacts within butterflies. A nice fit of the data was accomplished with $J1$ = 7.6 cm^{-1}, $J2$ = −22.4 cm^{-1}, and g = 2.42, neglecting all Ni...Ni contacts not having a monatomic bridge. Here, the lower Ni−O−Ni angle in the range of 93−99° generates ferromagnetic interactions via $J1$, whereas the Ni−O−Ni angle in the range of 111−135° generates antiferromagnetic interaction as discussed for compound **3**.[24,27]

dx.doi.org/10.1021/ic402673v | Inorg. Chem. 2014, 53, 1606−1613

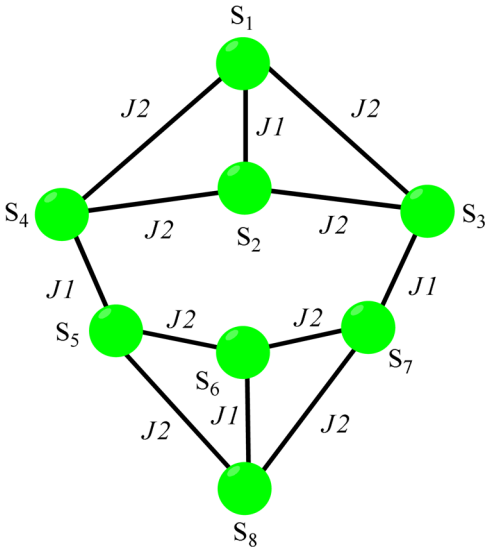

Figure 14. Models used for the data fitting of compound **4**. Balls represent metal centers and lines represent connectivity between two metal centers.

$$\mathbf{H} = -J1(S_1S_2 + S_3S_7 + S_4S_5 + S_6S_8) - J2(S_1S_3 + S_1S_4 + S_2S_3 + S_2S_4 + S_5S_6 + S_6S_7 + S_5S_8 + S_7S_8) - g\mu\mathbf{B}H.\sum_{i=1}^{8} S_i \quad (2)$$

The room-temperature $\chi_M T$ value of 36.15 cm^3 K mol^{-1} for compound **5** can be explained after taking the orbital contribution of Co^{II} in an octahedral field into consideration.[8e,26] The $\chi_M T$ value decreases gradually from room temperature to 29.23 cm^3 K mol^{-1} for compound **5** at 80 K and then sharply to 2.36 cm^3 K mol^{-1} at 1.8 K (Figure 15). Because

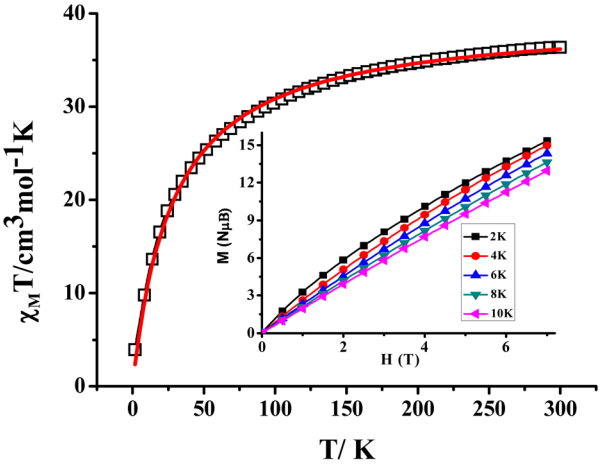

Figure 15. Temperature dependence of $\chi_M T$ measured at 0.1 T. The red solid line is the best fit obtained. Magnetization curves (inset graphs) measured at 2−10 K for complex **5**.

of the orbital contribution in the $\chi_M T$ value, we were unable to fit the experimental data. However, the data were well-fitted over the temperature range of 1.8−300 K with the Curie equation, which gives C = 39.55(6) cm^3 mol^{-1} K and θ = −28.28(5) K. The negative θ value indicates the presence of moderate antiferromagnetic interactions in the structure. The magnetization plot shows no sign of saturation even at higher fields as in compounds **1** and **2** and can be understood on similar grounds.

CONCLUSION

Exploring symmetry and the regular geometry of paramagnetic cores is very important in terms of understanding the magnetic properties of the molecular systems. We have reported the synthesis and the structural and magnetic properties of five high-nuclearity transition-metal phosphonate cages, and an attempt has been made to explore the geometry and symmetry present in the core of the serendipitously formed compounds. It is also noticed that the structure of the phosphonate cages is strongly affected by the reaction conditions and/or the involvement of additional coligand. Magnetic studies confirm the coexistence of both antiferromagnetic and ferromagnetic interactions between the metal centers in all cases. Presently, we are trying to isolate different nuclearity cages with Co and Ni under ambient conditions and exploring the effect of coligand under different reaction conditions.

ASSOCIATED CONTENT

Supporting Information

BVS calculations, PXRD and TGA plots, table of magnetic measurements. This material is available free of charge via the Internet at http://pubs.acs.org.

AUTHOR INFORMATION

Corresponding Author

*E-mail: skonar@iiserb.ac.in.

Notes

The authors declare no competing financial interest.

ACKNOWLEDGMENTS

J.A.S. and A.A. acknowledge CSIR for their JRF fellowship. S.B. thanks IISER, Bhopal for the Ph.D. fellowship. H.S.J. thanks IISER, Bhopal for post-doctoral fellowship. S.K. thanks DST, Government of India (Project No. SR/FT/CS-016/2010), and IISER Bhopal for generous financial and infrastructural support.

DEDICATION

Dedicated to Professor R. N. Mukherjee on the occasion of his 60th birthday.

REFERENCES

(1) (a) Zheng, Y. Z.; Evagelisti, M.; Tuna, F.; Winpenny, R. E. P. *J. Am. Chem. Soc.* **2012**, *134*, 1057−1065. (b) Zheng, Y. Z.; Pineda, E. M.; Helliwell, M.; Winpenny, R. E. P. *Chem.—Eur. J.* **2012**, *18*, 4161−4165. (c) Thompson, M. E. *Chem. Mater.* **1994**, *6*, 1168−1175. (d) Sessoli, R.; Gatteschi, D.; Caneschi, A.; Novak, M. A. *Nature* **1993**, *365*, 141−143. (e) Thomas, L.; Lionti, F.; Ballou, R.; Gatteschi, D.; Sessoli, R.; Barbara, B. *Nature* **1996**, *383*, 145−147.

(2) (a) Taft, K. L.; Papaefthymiou, G. C.; Lippard, S. J. *Science* **1993**, *259*, 1302−1305. (b) Theil, E. C.; Matzapetakis, M.; Liu, X. J. J. *Biol. Inorg. Chem.* **2006**, *11*, 803−810. (c) Lee, S. C.; Holm, R. H. *Chem. Rev.* **2004**, *104*, 1135−1158.

(3) (a) Müller, A.; Sarkar, S.; Shah, S. Q. N.; Bögge, H.; Schmidtmann, Sh.; Sarkar, M.; Kögerler, P.; Hauptfleisch, B.; Trautwein, A.; Schünemann, V. *Angew. Chem., Int. Ed. Engl.* **1999**, *38*, 3238−3241. (b) Müller, A.; Todea, A. M.; Bögge, H.; Slageren, J. V.; Dressel, M.; Stammlera, A.; Rusu, M. *Chem. Commun.* **2006**, 3066−3068. (c) Müller, A. *Nature* **1991**, *352*, 115−116.

(4) (a) Gatteschi, D.; Sessoli, R. *Angew. Chem., Int. Ed.* **2003**, *42*, 268−297. (b) Glaser, T. *Chem.Comm.* **2011**, *47*, 116−130. and

references therein. (c) (g) Konar, S.; Mukherjee, P. S.; Zangrando, E.; Lloret, F.; Ray Chaudhuri, N. *Angew. Chem., Int. Ed.* **2002**, *41*, 1561−1563. (d) Gomez-Coca, S.; Cremades, E.; Aliaga-Alcalde, N.; Ruiz, E. *J. Am. Chem. Soc.* **2013**, *135*, 7010−7018.
(5) (a) Abu-Nawwas, A.-A. H.; Mason, P. V.; Milway, V. A.; Muryn, C. A.; Pritchard, R. J.; Tuna, F.; Collison, D.; Winpenny, R. E. P. *Dalton Trans.* **2008**, *2*, 198−200. (b) King, P.; Stamatatos, T. C.; Abboud, K. A.; Christou, G. *Angew. Chem., Int. Ed.* **2006**, *45*, 7379−7383. (d) Brechin, E. K.; Cador, O.; Caneschi, A.; Cadiou, C.; Harris, S. G.; Parsons, S.; Vonci, M.; Winpenny, R. E. P. *Chem. Commun.* **2002**, 1860−1861.
(6) (a) Glaser, T.; Liratzis, I.; Ako, A. M.; Powell, A. K. *Coord. Chem. Rev.* **2009**, *253*, 2296−2305. (b) Goodwin, J. C.; Sessoli, R.; Gatteschi, D.; Wernsdorfer, W.; Powell, A. K.; Heath, S. L. *J. Chem. Soc., Dalton Trans.* **2000**, 1835−1840. (c) Baniodeh, A.; Hewitt, I. J.; Mer.eacre, V.; Lan, Y.; Novitchi, G.; Anson, C. E.; Powell, A. K. *Dalton Trans.* **2011**, *40*, 4080−4086.
(7) (a) Clearfield, A. Metal Phosphonate Chemistry. In *Progress in Inorganic Chemistry*; Karlin, K. D., Ed.; John Wiley & Sons: New York, 1998; p 371 and references therein. (b) Clearfield, A.; Wang, Z. *Dalton Trans.* **2002**, 2937−2947.
(8) (a) Maheswaran, S.; Chastanet, G.; Teat, S. J.; Mallah, T.; Sessoli, R.; Wernsdorfer, W.; Winpenny, R. E. P. *Angew. Chem., Int. Ed.* **2005**, *44*, 5044−5048. (b) Tolis, E. I.; Helliwell, M.; Langley, S.; Raftery, J.; Winpenny, R. E. P. *Angew. Chem., Int. Ed.* **2003**, *42*, 3804−3808. (c) Zheng, Y. Z.; Evangelisti, M.; Winpenny, R. E. P. *Angew. Chem., Int. Ed.* **2011**, *50*, 3692−3695. (d) Brechin, E. K.; Coxall, R. A.; Parkin, A.; Parsons, S.; Tasker, P. A.; Winpenny, R. E. P. *Angew. Chem., Int. Ed.* **2001**, *40*, 2700−2703. (e) Zheng, Y.; Evangelisti, M.; Winpenny, R. E. P. *Chem. Sci.* **2011**, *2*, 99−102. (f) Langley, S.; Helliwell, M.; Teat, S. J.; Winpenny, R. E. P. *Dalton Trans.* **2012**, *41*, 12807−12817. (g) Langley, S.; Helliwell, M.; Sessoli, R.; Teat, S. J.; Winpenny, R. E. P. *Dalton Trans.* **2009**, 3102−3110. (h) Langley, S.; Helliwell, M.; Sessoli, R.; Teat, S. J.; Winpenny, R. E. P. *Inorg. Chem.* **2008**, *47*, 497−507. (i) Langley, S.; Helliwell, M.; Sessoli; Rosa, P.; Wernsdorfer, W.; Winpenny, R. E. P. *Chem. Commun.* **2005**, 5029−5031. (j) Pineda, E. M.; Tuna, F.; Zheng, Y. Z.; Winpenny, R. E. P.; McInnes, E. J. L. *Inorg. Chem.* **2013**, *52*, 13702−13707.
(9) (a) Konar, S.; Bhuvanesh, N.; Clearfield, A. *J. Am. Chem. Soc.* **2006**, *128*, 9604−9605. (b) Konar, S.; Clearfield, A. *Inorg. Chem.* **2008**, *47*, 3489−3491. (c) Konar, S.; Clearfield, A. *Inorg. Chem.* **2008**, *47*, 5573−5579. (d) Houston, P.; Jerzy, Z.; Justin, L.; Clearfield, A. *J. Solid State Chem.* **2010**, *183*, 1165−1173.
(10) (a) Chandrasekhar, V.; Kingsley, S. *Angew. Chem., Int. Ed.* **2000**, *39*, 2320−2322. (b) Chandrasekhar, V.; Nagarajan, L.; Clerac, R.; Ghosh, S.; Verma, S. *Inorg. Chem.* **2008**, *47*, 1067−1073. (c) Chandrashekhar, V.; Dey, A.; Senapati, T.; Sanudo, E. C. *Dalton Trans.* **2012**, *41*, 789−803. (d) Chandrashekhar, V.; Sahoo, D.; Suriyanarayanan, R.; Butcher, R. J.; Lloret, F.; Pardo, E. *Dalton Trans.* **2013**, *42*, 8192−8196. (e) Chandrashekhar, V.; Dey, A.; Senapati, T.; Hossain, S. *Dalton Trans.* **2011**, *40*, 5394−5418 and references therein.
(11) (a) Walawalker, M. G.; Roesky, H. W.; Murugavel, R. *Acc. Chem. Res.* **1999**, *32*, 117−126. (b) Yao, H. C.; Li, Y. Z.; Song, Y.; Ma, Y. S.; Zheng, L. M.; Xin, X. Q. *Inorg. Chem.* **2006**, *45*, 59−65. (c) Yang, C. I.; Song, Y. T.; Yeh, Y. J.; Liu, Y. H.; Tseng, T. W.; Lu, K. L. *CrystEngComm.* **2011**, *13*, 2678−2686. (d) Speed, S.; Vicente, R.; Aravena, D.; Ruiz, E.; Roubeau, O.; Teat, S. J.; Fallah, M. S. E. *Inorg. Chem.* **2012**, *51*, 6842−6850. (e) Wayne, O.; Zubeita, J. *ACS Symposium Series.* **2007**, *974*, 392−407. (f) Wayne, O.; Guangbin, W.; Hongxue, L.; Gordon, T.; Charles, J.; Zubieta, J. *Inorg. Chem.* **2009**, *48*, 953−963.
(12) (a) Zhang, L.; Clerac, R.; Heijboer, P.; Schmitt, W. *Angew. Chem., Int. Ed.* **2012**, *51*, 3007−3011.
(13) (a) Sheikh, J. A.; Goswami, S.; Adhikary, A.; Konar, S. *Inorg. Chem.* **2013**, *52*, 4127−4129. (b) Sheikh, J. A.; Jena, H. S.; Adhikary, A.; Khatua, S.; Konar, S. *Inorg. Chem.* **2013**, *52*, 9717−9719.
(14) (a) Harvey, R. G.; Desombre, E. R. *Top. Phosphorus Chem.* **1964**, *1*, 57−111. (b) Redmore, D. *J. Org. Chem.* **1976**, *41*, 2148−2150.
(15) Liu, W.; Thorp, H. H. *Inorg. Chem.* **1993**, *32*, 4102−4105.
(16) SAINT: *SAX Area-Detector Integration Program*, v6.22; Bruker AXS Inc.: Madison, WI, 1997−2001.
(17) Sheldrick, G. SADABS, *Program for Absorption Correction of Area Detector Frames*; Bruker AXS Inc.: Madison, WI, 2008.
(18) Sheldrick, G. *SHELXL-97, Program for Crystal Structure Refinement*; University of Gottingen: Gottingen, Germany, 1997.
(19) PLATON: Speck, A. L. *J. Appl. Crystallogr.* **2003**, *36*, 7−13.
(20) Speck, A. L. PLATON. Molecular Geometry Program. *J. Appl. Crystallogr.* **2003**, *7*.
(21) Aromi, G.; Batsanov, A. S.; Christian, P.; Helliwell, M.; Parkin, A.; Parsons, S.; Smith, A. A.; Timco, G. A.; Winpenny, R. E. P. *Chem.—Eur. J.* **2003**, *9*, 5142−5161.
(22) Chaboussant, G.; Basler, R.; Gudel, H. U.; Ochsenbein, S. T.; Parkin, A.; Parsons, S.; Rajaraman, G.; Sieber, A.; Smith, A. A.; Timco, G. A.; Winpenny, R. E. P. *Dalton Trans.* **2004**, 2758−2766.
(23) Coxall, R. A.; Harris, S. G.; Henderson, D. K.; Parsons, S.; Tasker, P. A.; Winpenny, R. E. P. *J. Chem. Soc., Dalton Trans.* **2000**, 2349−2356.
(24) Breeze, B. A.; Shanmugam, M.; Tuna, F.; Winpenny, R. E. P. *Chem. Commun.* **2007**, 5185−5187.
(25) Engelhardt, L.; Luban, M. *Dalton Trans.* **2010**, *39*, 4687−4692.
(26) Ma, Y. S.; Song, Y.; Tang, X. Y.; Yuan, R. X. *Dalton Trans.* **2010**, *39*, 6262−6265.
(27) Kahn, O. *Molecular Magnetism*; VCH: New York, 1993. (b) Clemente-Juan, J. M.; Chansou, B.; Donnadieu, B.; Tuchagues, J. P. *Inorg. Chem.* **2000**, *39*, 5515−5519.